

Contents list available at CBIORE journal website

International Journal of Renewable Energy Development

Journal homepage: https://ijred.cbiore.id



Research Article

Energy potential of biochar from slow pyrolysis of mixed tree leaves in a pilot-scale fixed-bed reactor

Segun E. Ibitoye^{a,b}, Meraj Alam^{c,d}, Olalekan A. Olayemi, Esther T. Akinlabi Ishita Sarkar^c, Rasheedat M. Mahamood^{gh}, Tien-Chien Jen^h, Chanchal Loha^c

Abstract. Thermochemical conversion processes, such as pyrolysis, offered significant potential for harnessing energy from biomass as a substitute for conventional fuels. This study investigated energy generation from mixed tree leaves through pyrolysis. The pyrolysis was conducted at 3 temperatures: 400, 500, and 600 °C. Characterization of the feedstock and pyrolysis products was carried out following international standards. The results showed that bio-oil yields (26.13–39.95%) and syngas yields (30.33–39.38%) increased with temperature, while the char yield decreased from 43.66-29.67%. The FC VM, AC, and MC of the biochars varied from 61.26-67.71, 4.58-12.75, 21.32-25.32, and 2.39-4.67%, respectively. After pyrolysis, the highest C (67.71%) was obtained at 600 °C, while the highest H (3.98%) was recorded at 400 °C. The study revealed that FC, AC, and C increased with temperature, whereas MC, VM, H, and O decreased. The produced biochars, particularly Char₆₀₀, demonstrated HHV values (up to 23.32 MJ/kg), improved FC, and enhanced BET surface areas. While slightly lower than the HHV of traditional metallurgical coke, the biochars showed strong potential for partial substitution or co-injection in high-temperature metallurgical processes. The enhanced porosity and C contribute to their suitability as renewable solid fuels, supporting carbon footprint reduction in heavy industries.

Keywords: Biochar, Biomass energy, Slow pyrolysis, Fixed bed Reactor, Mixed tree leaves, Thermochemical conversion.



@ The author(s). Published by CBIORE. This is an open access article under the CC BY-SA license (http://creativecommons.org/licenses/by-sa/4.0/). Received: 21st March 2025; Revised: 25th June 2025; Accepted: 10th July 2005; Available online: 22nd July 2025

1. Introduction

The effects of fossil fuel consumption on human health, the natural world, and the environment cannot be overstated, including rising global average temperatures, global warming, and emissions of greenhouse gases (Fraia et al., 2023; Mu et al., 2023). This is because of excessive reliance on petroleum and petroleum derivatives as a key energy source. Population growth and rising energy usage have also prompted several environmental challenges. Consequently, in establishing the goals for 2030, the United Nations has made providing environmentally friendly energy one of its top priorities (UN, 2024). Thus, there has been an increase in sustainable and alternative energy research in recent years. Renewable energy sources include hydro, thermal, tidal, biomass, wind, and solar (Ibitoye et al. 2021b). Among the alternative energy sources, biomass demonstrated sustainable and attractive properties. This is because of the great number of biomass in many forms, including wood and wood residues, and non-woody, such as agro-waste (Ibitoye et al., 2023). Biomass is classified as a zerocarbon energy source since the carbon emitted throughout energy usage is nearly balanced by the carbon absorbed during growth. As a result, widespread use has the potential to cut harmful emissions.

Forest residues like tree leaves must be appropriately treated to minimize the environmental effects of their dumping and burning in open fields, and to be efficiently converted into usable energy. This addresses several drawbacks related to unprocessed biomass, like low thermal performance, low energy and bulk densities, high moisture content, and difficulties with sustainability, logistics, and preservation (Ibitoye et al. 2024; Ibitoye et al. 2021a). Several approaches have been proposed to address the shortcomings of biomass for

^aSchool of Technology, Woxsen University, Kamkole, Sadasivpet, Sangareddy District, Hyderabad-500033, India.

bDepartment of Mechanical Engineering, Faculty of Engineering and Technology, University of Ilorin, P. M. B. 1515, Ilorin, Nigeria.

^cEnergy Research and Technology Group, CSIR-Central Mechanical Engineering Research Institute, Durgapur, West Bengal, India.

^dAcademy of Scientific and Innovative Research (AcSIR), Ghaziabad-201002, India.

Department of Aeronautics and Astronautics, Faculty of Engineering and Technology, Kwara State University, Malete, Kwara State, Nigeria.

^fDepartment of Mechanical Engineering, Colorado State University, Fort Colins, USA.

^{*}Department of Mechanical and Construction Engineering, Faculty of Engineering and Environment, Northumbria University, Newcastle NE1 8ST, United Kingdom.

hDepartment of Mechanical Engineering Science, Faculty of Engineering and the Built Environment, University of Johannesburg, P. O. Box 524, Auckland Park 2006, South Africa

Corresponding author Email: ibitoye.s@unilorin.edu.ng (S.E.Ibitoye)

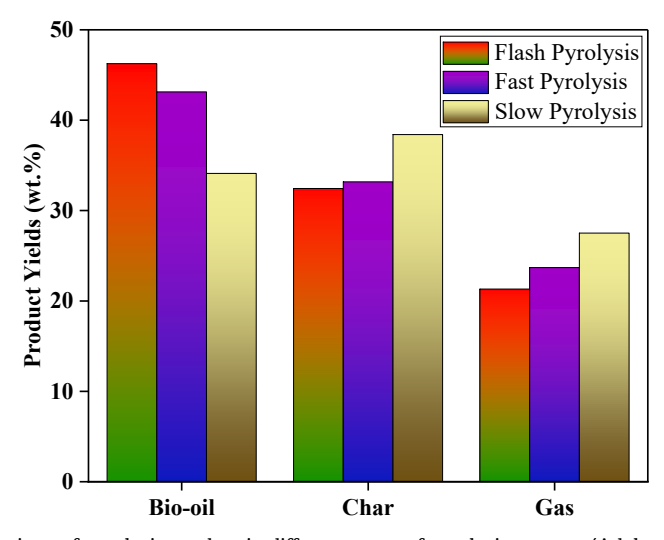


Fig. 1 Comparison of pyrolysis product in different types of pyrolysis process (Adelawon et al., 2021)

Table 1General operating conditions for different types of pyrolysis (Gabbar & Aboughaly, 2021)

Pyrolysis type	Residence time	Heating Rate (°C/s)	Temp. Range (°C)	Energy Input	Reliability/ Complexity
Slow	10-100 min	0.1-1	300-700	Intermediate	Simple/Reliable
Fast	0.5-5 s	10-200	400-800	High	Complex
Flash	<0.5 s	>1000	800-1000	Higher	More Complex

energy-related purposes. These involve thermal (Cormos, 2023: Lahiri et al., 2023; Arivanti et al, 2024), biological (Adekunle et al., 2019), mechanical (Ibitoye et al., 2023), and physical (Ibitoye et al., 2021) processing. The thermal processing procedure involves heating feedstock in an inert environment. Thermal processing includes torrefaction, pyrolysis, gasification, carbonization, etc (Huang et al., 2016; Yang et al., 2007; Yiga et al., 2023; Haniif et al., 20204). Thermal treatment increases the combustibility characteristics of biomass. Residence time, heating rate, temperature, catalytic activities, and particle sizes have all been proven to influence thermally treated products (Alam et al., 2024; Zhao et al., 2017). However, the most important parameters are residence time, temperature, and heating rate.

Understanding the thermochemical decomposition characteristics of different biomass feedstocks is essential for optimizing the decomposition process. Leaves generated by trees are abundant and, most of the time, underutilized. Tree leaves can be a renewable energy source when properly processed and converted into biofuels via thermochemical processes such as pyrolysis (Mudryk et al., 2021; Rajendra et al., 2019). Pyrolysis transforms the leaf feedstock into usable energy and other useful products by heating it in an inert environment (Christwardana et al 2025). It converts the biomass feedstock of biomass into three products- solid (char), condensable liquid (bio-oil), and non-condensable gas (syngas) in the absence of oxygen. Biomass may be pyrolyzed using various methods, including slow, flash, traditional, and fast pyrolysis (Abdullah et al., 2023; A. Gupta et al., 2021; Haniif et al, 2024). Although each pyrolysis process has unique characteristics corresponding to its temperature, heating rate, or type of reactor, the subsequent change in product yield percentage is also observed. This research focuses on analyzing the characteristics of pyrolysis products for renewable hydrogen production and exploring alternatives to coal for iron and steel applications. From Fig. 1 and Table 1, it can be observed that slow pyrolysis consumes less energy input (Adelawon et al., 2021) as compared to fast and flash pyrolysis and produces more amount of syngas and

char as compared to others. As a result, a slow pyrolysis technique is selected for this study.

This study examines the possibility of transforming tree wastes/residues (leaves) into usable energy. This study is important as it proposes renewable energy solutions, advances waste management initiatives, and provides eco-friendly advantages by minimizing GHG emissions. Furthermore, the produced biochar can serve as an alternative to coke and coal in iron and steel-making. The research also contributes to advanced pyrolysis technology and systems.

There are some knowledge gaps that this study seeks to address. There is limited study on the detailed energy potential of mixed tree leaves as a renewable energy source. There is a necessity to investigate the conversion of this feedstock to usable energy and maximize yield and quality for possible application in domestic and industrial settings, such as the iron and steel industries. In addition, comparative analyses with other carbon sources and assessments of their alternative potential for domestic and industrial use are conducted. This study seeks to fill these knowledge gaps, advancing the global pursuit of a sustainable future and aligning with the United Nations Sustainable Development Goals (SDGs). The findings of this study would advance the understanding of biomass pyrolysis and pave the way for developing practical and scalable solutions for sustainable energy production.

2. Methodology

2.1. Material collection and preparation

The biomass used in this study was mixed tree leaves (MTL) and was selected based on abundance, accessibility, real-world relevance, underutilized but valuable, and energy potential. MTL represents a *heterogeneous*, *abundant biomass stream*, especially in tropical and subtropical regions. Unlike agro-waste, which is crop-dependent and seasonal, tree leaves are shed continuously and predictably in institutional (such as the CSIR-CMERI campus), residential, urban, and rural areas. This constant availability reduces supply volatility, enabling



Fig. 2 Biomass sample- (a) raw sample and (b) pulverized sample

year-round renewable energy generation. Additionally, MTL better simulates *real-world waste biomass streams* encountered in municipal solid waste systems compared to single-species feedstocks, aligning with practical large-scale pyrolysis applications. Previous studies showed that leaf-based biomass can yield biochars with competitive properties, validating their viability (Adeniyi *et al.*, 2024; Antonangelo *et al.*, 2025; Khater *et al.*, 2024; Putri *et al.*, 2023; Ong *et al.* 2024; Satomi *et al.*, 2025). Commonly burned or discarded, MTL presents an opportunity for sustainable waste valorization and decentralized renewable energy.

The MTL samples were collected from the CSIR-CMERI Colony, Durgapur, India. The collected biomass samples were sorted from unwanted materials such as sand, stones, paper, nylon grasses, etc., and sun-dried for 96 h. The dried samples were conditioned in an electric oven at 120 °C for 2 h, after which they were kept in zip-lucked bags for further characterization (Basu, 2010). The picture of the raw and pulverized biomass is shown in Fig. 2.

2.2. Methods

2.2.1. Pyrolysis experiment

The study adopted the pyrolysis setup and experimental procedure outlined by Alam *et al.* (2024), maintaining isothermal conditions throughout. Each experiment involved charging 300 g of feedstock into the reactor, gradually heating it to the desired temperature in 30 minutes, and then maintaining it for 2 hours. Pyrolysis was carried out at three temperatures (400, 500, and 600 °C). The maximum pyrolysis temperature was set

at 600 °C based on the results from the thermogravimetric analysis (TGA), which revealed that temperature has no significant effect on mass loss beyond 600 °C.

During pyrolysis, biomass was converted into biochar, while the vapors were condensed into bio-oil. The non-condensable gases generated were purified using isopropyl alcohol. The biochar, syngas, and bio-oil were collected for further analysis. Each experiment was repeated 3 times, and average values were recorded. The diagrammatic representation of the pyrolysis setup is presented in Fig. 3.

2.3. Raw biomass and biochar characterization

2.3.1. Proximate analysis

The proximate experiment of the biomass and pyrolyzed biochar was carried out to quantify the proportion of volatile matter (VM), moisture (MC), ash (AC), and fixed carbon (FC) contents of the samples. A Muffle furnace was used to determine the proximate parameters of biomass and biochar.

MC was calculated in accordance with ASTM standards (ASTM E177-19, 2019). A weighted sample (W_a) was placed in crucible. With the crucible opened, the sample was transferred into an oven regulated at $107\pm3^{\circ}$ C for 1 hour. The sample was retrieved from the oven, covered, and placed in a desiccator to cool down. After sufficient cooling, the weight (W_b) of the sample was determined and recorded. The proportion of MC was estimated using Equation 1.

Moisture content (MC) =
$$\frac{W_a - W_b}{W_a} \times 100$$
 (1)

The VM was calculated based on the ASTM method (ASTM D3175-11, 2013). After the MC determination, the same weighted sample was placed in a crucible with the lid closed. The sample in the closed crucible was then placed in a Muffle furnace at 950 °C for 7 minutes. After 7 minutes, the sample was retrieved from the furnace and cooled for about 10 minutes, after which it was transferred into a desiccator for further cooling to ambient. The weight (W_c) of the sample was measured after sufficient cooling. Equation 2 was used to compute the volatile matter content.

Volatile matter (VM) =
$$\frac{W_b - W_c}{W_a} \times 100$$
 (2)

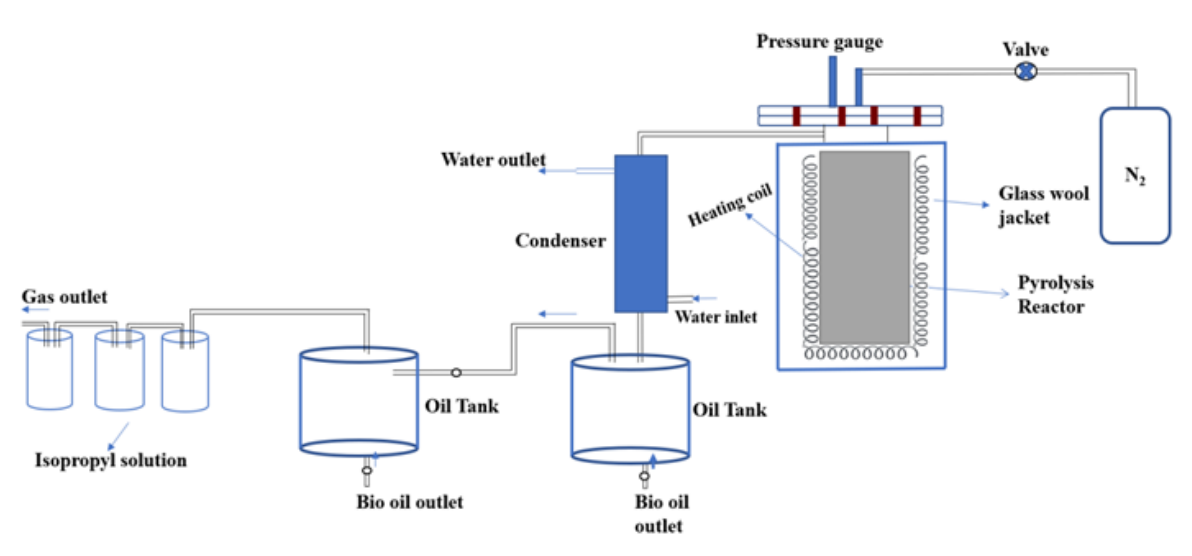


Fig. 3 Diagrammatical representation of the pilot-scale pyrolysis setup (Alam et al., 2024)

The AC was calculated following the ASTM E1755-01 (2015) standard. After computing the proportion of VM, the weighted sample with the crucible open was kept in the Muffle furnace at 600 °C for 3 h. The sample was collected after 3 h and cooled in the desiccator to room temperature. The weight (W_d) of the sample was measured and recorded. The AC was computed using Equation 3, while the FC was calculated using Equation 4.

Ash content (AC) =
$$\frac{W_d}{W_a} \times 100$$
 (3)

$$FC = 100 - (MC + VM + AC)$$
 (4)

2.3.2. Elemental analysis

The Carbon (C), Hydrogen (H), and Oxygen (O) were determined using the correlation Equations 5, 6, and 7, respectively, given by Parikh *et al.* (2007).

$$C = 0.637FC + 0.455VM (5)$$

$$H = 0.052FC + 0.062VM \tag{6}$$

$$C = 0.304FC + 0.476VM \tag{7}$$

2.3.3. Higher heating value (HHV)

The biomass's HHV was determined using a bomb calorimeter setup IKA C 3000 ISOPERIBOL calorimeter.

2.3.4. Thermogravimetric analysis (TGA)

The thermal breakdown of the biomass and biochar was studied using a thermogravimetric analyzer, NETZSCH-Geratebau GmbH, and model 209 F3 Tarsus. The TGA was performed at a 10 K/min heating rate in a Nitrogen environment. The experiment was conducted at a temperature range of 30-700 °C, while 40 mL/min was adopted as the nitrogen flow rate.

2.3.5. Fuel ratio and degree of pyrolysis

Fuel ratio (F_r) provides insight into the relative quantities of FC and VM in fuel, while the degree of pyrolysis (d_p) reveals the level of decomposition that the biomass samples have undergone after heating in an inert environment. The F_r and d_p were respectively determined using Equations 8 and 9 (Ibitoye *et al.* 2021b).

$$F_r = \frac{FC}{VM} \tag{8}$$

$$d_p = \frac{VM_{biochar}}{VM_{Raw\ biomass}} \tag{9}$$

2.3.6. Energy density, enhancement factor, and energy yield

The enhancement factor (E_f) , energy yield (E_y) , and density (E_d) of the biomass was calculated using Equations 10, 11, and

12, respectively (Ibitoye et al. 2021b; Kongto et al. 2021; Singh, Sarkar, and Chakraborty 2019).

$$E_f = \frac{HHV_{biochar}}{HHV_{Raw\ Biomass}} \tag{10}$$

$$E_{y} = (Biochar\ yeild) \times \frac{HHV\ _{biochar}}{HHV\ _{Raw\ Biomass}}$$
(11)

2.3.7. Compressibility index

Carr's compressibility index (*CCI*) was employed to study the compressibility behavior of biochar. This was determined from the tapped and bulk density of biochar using Equation 13. Equation 14 was adopted to determine the Hausner ratio (Magasiner *et al.*, 2002; S. Singh *et al.*, 2020).

$$CCI = \left(\frac{Tapped\ Density - Bulk\ Density}{Tapped\ Density}\right) \times 100 \tag{12}$$

$$HR = \frac{Tapped\ Density}{Bulk\ Density} \tag{13}$$

2.3.8. Morphological characteristics

The raw biomass and biochar's morphological characteristics were studied using FESEM-EDS (Zeiss, Model: Gemini 300). Specifically, the properties investigated include surface morphology, elemental composition, raw biomass, and biochar.

3. Results and discussion

The results of the thermal and combustion characterization were presented and discussed in this section.

3.1. Proximate analysis and elemental analysis

The proximate characterization results of the biochars and raw biomass are shown in Table 2. The MC and VM of the biochars varied from 2.39-4.67 and 19.32-14.32, respectively, while the FC and AC varied from 65.26-78.71 and 4.58-10.75%, respectively. The MC, AC, VM, and FC of the raw biomass are 10.60, 5.85, 68.89, and 14.66, respectively. Analyses of the results revealed that the percentage of FC and AC increases with temperature, while MC and VM decrease. This observation aligned with the results of Oginni and Singh (2019), which that thermal treatment decomposed explained hemicellulose, cellulose, and lignin constituents of biomass, resulting in the emission of VM, loss of MC, and an enhanced FC. The increase in ash content with temperature reflects the concentration effect. As volatiles are released, the noncombustible mineral components of the biomass (like silica, potassium, calcium, and other inorganic compounds) remain in the solid phase, causing the ash content to increase. Thus, at higher pyrolysis temperatures, the relative proportion of ash increases because the organic matter has largely decomposed

 Table 2

 Proximate and elemental parameters of pyrolyzed and raw biomass

Sample ID	Proximate			Ultimate			
	MC	AC	VM	FC	С	Н	0
Char ₄₀₀	4.67	19.32	10.75	65.26	63.13	3.98	21.43
Char ₅₀₀	3.86	17.62	6.76	71.76	68.43	2.87	17.25
Char ₆₀₀	2.39	14.32	4.58	78.71	76.31	2.13	10.76
Raw Biomass	10.6	5.85	68.89	14.66	47.04	4.86	46.13

and volatilized. Several researchers have reported similar patterns using different biomass feedstocks (Asadi Zeidabadi *et al.*, 2018; De Bhowmick *et al.*, 2018).

The proximate properties of the MTL biochars produced in this study show notable differences when compared to agricultural waste biochars reported by Durango Padilla et al. (2024). The FC of Char₆₀₀ (78.71%) is comparable to that of coconut shell (79.4%) and corncob (80.0%) biochars produced at 500 °C, and significantly higher than that of eucalyptus bark biochar (58.2%). This result suggests that MTL, when pyrolyzed under optimized conditions, can yield solid fuels with competitive carbon richness essential for high-temperature applications. The higher AC observed in this study (14.32-19.32%) compared to coconut-shell and corncob biochars (approximately 5–6%) can be scientifically attributed to the inherent mineral matter in leaf-based biomass. Tree leaves typically accumulate minerals (e.g., potassium, calcium, magnesium) from the soil during growth, leading to higher ash formation during pyrolysis (Khater et al., 2024; Oyebamiji et al., 2025).

Additionally, the significantly lower VM in the mixed leaves biochars (Char₆₀₀: 4.58%) relative to coconut-shell and corncob biochars (14.4–15%) indicates more extensive devolatilization and higher thermal stability (Durango Padilla *et al.*, 2024). This can be linked to the heterogeneous structure of MTL. Furthermore, variations in pyrolysis conditions — such as residence time and heating rate— also contribute to the observed differences. For instance, slow heating rates and extended residence times promote secondary char formation reactions, leading to higher fixed carbon and lower volatile matter fractions (Babu *et al.*, 2024).

The characterization of the raw biomass showed C of 47.04%, H of 4.86%, and O of 4.86%. After pyrolysis, the highest C (76.31%) and H (3.98%) were displayed by Char₆₀₀ and Char₄₀₀, samples, respectively. Analysis of the results showed that the C of the char increases with temperature while the H and O decrease. This trend is primarily due to dehydration, decarbonylation, and decarboxylation processes. Dehydration reactions occur early on, removing water molecules (H2O) from the biomass structure and reducing the hydrogen and oxygen content, thereby concentrating the carbon. As temperatures rise further, decarbonylation reactions release carbon monoxide (CO), and decarboxylation reactions release carbon dioxide (CO₂). Both processes contribute to a significant reduction in oxygen relative to carbon. The cumulative effect of these reactions results in the progressive enrichment of carbon in the char, as hydrogen and oxygen are volatilized and lost in gaseous forms (Oginni & Singh, 2019).

3.2. Van Krevelen Diagram

A fundamental tool for evaluating the suitability of solid fuels for energy applications is the Van Krevelen diagram, and it is the H/C vs. O/C atomic ratios (Fig. 4). The atomic ratios of the produced biochar decrease with increasing pyrolysis temperature, ranging from 0.339-0.141(H/C) and 0.063-0.027 (O/C). In comparison, the corresponding values for the raw biomass are 0.981 and 0.103. The results indicate that the biochar produced in this study compares favorably with coal, which typically exhibits an O/C ratio of 0.06281-0.19163 and an H/C ratio of 0.077281-0.08733 (Loo & Koppejan, 2008; Trif-Tordai & Ionel, 2011). Biochar produced from MTL can be classified as moderate to high-quality fuel. The reduction in atomic ratios with temperature is due to the depletion of hydrogen and oxygen, which enhances carbon aromaticity. This process occurs as O- and H-containing functional groups break

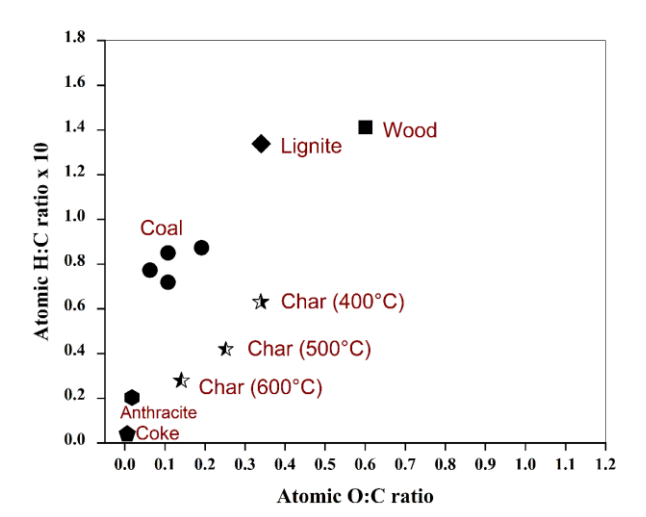


Fig. 4 Comparison between the atomic ratio of the produced char with other conventional solid fuels

down, yielding char with increased aromatic characteristics and reduced polarity at higher temperatures (Wu et al., 2019).

Irfan et al. (2016) opined that O/C and H/C ratios decrease with temperature while characterizing the biochar produced from Achnatherum splendens. The decline in these atomic ratios at elevated temperatures is mainly attributed to dehydration and decarboxylation reactions. Additionally, Spokas (2010) highlighted that a smaller O/C ratio signifies consistency in the carbon property of biochar. Notably, an O/C ratio below 0.2 suggests a biochar with a half-life of about 1000 years.

3.3. Elemental Analysis

The C, H, and O of the raw biomass are 40.04, 4.81, and 35.13%, respectively. After pyrolysis, the highest C (67.71%) and H (3.98%) were displayed by char generated at 600 °C (Char₆₀₀) and 400 °C (Char₄₀₀), respectively. It was discovered that the C of the char increases with temperature while the H and O decrease. It was observed that the C of the biochars was considerably higher than the raw biomass. This results from the dehydration, decarbonylation, and decarboxylation processes during pyrolysis (Oginni & Singh, 2019). The H/C ratio showed that the aromaticity index of the biochar decreases with an increase in temperature, which suggests an increase in carbon contents and biochar morphology comparable to graphite (Pariyar et al., 2020). Similarly, the O/C, a determinant for the biochar polarity, decreases with temperature. A smaller O/C ratio suggests fewer polar functional groups on the biochar's surface (Asadi Zeidabadi et al., 2018). The reduction in the O/C and H/C enhanced the combustion efficiency of the charreduction CO2, and smoke generation during the biochar burning.

The variations observed in the ultimate analysis results across the present study and those reported by Gupta *et al.* (2024), Satomi *et al.* (2025), and Adeniyi *et al.* (2023) can be attributed to several factors. Firstly, the type of feedstock plays a pivotal role. MTL, as used in the present study, inherently possesses a heterogeneous composition with varying lignin, cellulose, and hemicellulose contents. Lignin-rich biomasses tend to produce biochar with higher carbon content and lower oxygen content after pyrolysis, as lignin is more thermally stable and aromatizes during carbonization. This partially explains the higher carbon content (76.31% at 600 °C) observed for Char₆₀₀ compared to black currant leaves biochar (63.32%) reported by Satomi *et al.* (2025). Secondly, the pyrolysis conditions,

especially temperature, heating rate, and residence time, critically influence the extent of devolatilization and aromatic condensation. Slow pyrolysis at elevated temperatures promotes secondary char formation reactions, increasing fixed carbon content and decreasing hydrogen and oxygen fractions. This mechanism aligns with the progressive decrease in H and O contents observed in this study. Thirdly, the presence of inorganic components and external contaminants affects the elemental composition. For instance, Gupta *et al.* (2024) copyrolyzed leaf biomass with polypropylene (PP), introducing additional hydrogen-rich compounds, which increased the H/C atomic ratio compared to purely lignocellulosic biochars.

Environmental and soil conditions where the biomass is grown affect its initial chemical makeup, particularly the ashforming elements and mineral inclusions. Tree leaves often accumulate minerals such as potassium, calcium, and magnesium, which do not volatilize during pyrolysis and thus can influence both ash content and elemental oxygen retention. Methodological differences, such as whether empirical or direct elemental analysis methods are used, can introduce slight variations in reported values. In the present study, empirical estimation of CHO based on proximate analysis was adopted. While minor variations exist, the carbon-rich, low-hydrogen, and low-oxygen nature of the biochars produced from MTL is consistent with the broader characteristics required for high-temperature metallurgical applications and sustainable energy use (S. Gupta et al., 2024; Satomi et al., 2025).

3.4. Higher heating value (HHV)

A given fuel's energy and thermal properties are determined via the HHV. It is a vital indicator of fuel superiority and potential for energy production. The HHV of the untreated biomass and the biochar generated at different temperatures is shown in Fig. 5. It was discovered that the HHV of the biochar rises from 20.78-23.32 MJ/kg as the temperature increases from 400-600 °C. The increase in HHV with temperature is connected to the emission of VM and the increase in FC caused by the pyrolysis process. This observation aligned with previous findings that the HHV of biomass increases with treatment temperature. High-quality fuels must have elevated calorific values to obtain the most energy possible from solid fuels (Ahmed et al., 2020; Stylianou et al., 2020). Also, the results are consistent with the findings of Qiu et al. (2023), who reported that biochars derived from poplar tree leaves treated at higher pyrolysis temperatures (400-600 °C) exhibited improved HHVs, ranging from 18.2 to 21.2 MJ/kg. Similarly, Babu et al. (2024) observed that the HHVs of biochars produced from mixed wood waste and coconut husk waste varied between 24.65-27.92 MJ/kg and 21.32-23.63 MJ/kg, respectively, as the treatment temperature increased from 400 to 600 °C.

The HHV reported in the present study is higher than that of eucalyptus bark biochar (22.9 MJ/kg) but lower than that of coconut-shell (29.6 MJ/kg) and corncob (31.5 MJ/kg) biochars as reported by Durango Padilla et al. (2024). Such variations are primarily attributed to differences in biomass type and production methods. Further, the BET analysis presented in Section 3.10 revealed that Char₆₀₀ had a surface area of 17.36 m²/g, surpassing traditional carbon sources such as petroleum coke (0.95 m²/g), anthracite (0.71 m²/g), and bituminous coal (3.88 m²/g). This suggests enhanced reactivity and catalytic properties. According to Kieush et al. (2022), higher surface areas and pore volumes enable more efficient gas-solid reactions during iron reduction, partially compensating for lower HHV. Therefore, the produced biochars are suitable for partial substitution or co-injection with coke, particularly in reducing agents for metallurgical processes.

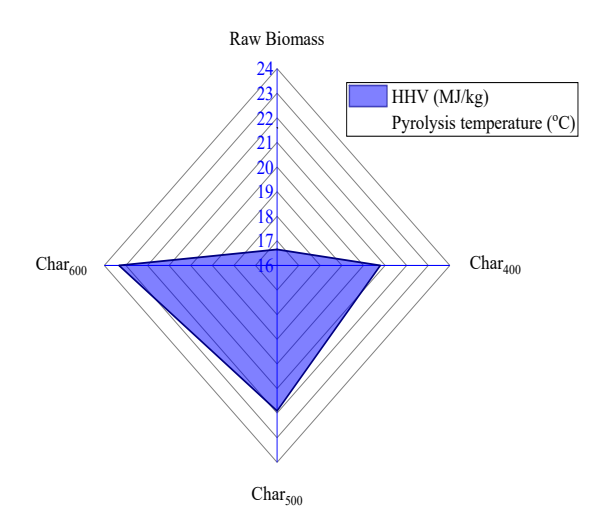


Fig. 5. Effect of temperature on HHV of the biomass

Although traditional metallurgical coke typically exhibits higher calorific values, recent studies have shown that full replacement with biochar is not necessary to achieve substantial performance gains. For instance, Babu et al. (2024) demonstrated that biochars with HHVs exceeding 20 MJ/kg, combined with high FC and favorable porosity, can serve as effective partial substitutes for coke in blast furnace injection processes. Similarly, Safarian (2023) reported that biochars with moderate HHVs but enhanced surface characteristics significantly contribute to the fuel mix without compromising furnace performance. Comprehensive data on the potential application of biochar across various iron and steelmaking processes can be found in the review by Al Hosni et al. (2024), which concluded that substitution levels ranging from 5-50% (typically 20–25%) are feasible, often without negatively impacting, and sometimes even improving, operational efficiency.

3.5. Thermogravimetric analysis

The TG graph of the raw biomass presented in Fig. 6a shows 3 different stages: dehydration (A), decomposition (B), and condensation (C) (Pattanayak et al., 2023; Pattanayak & Loha, 2023). The loss of moisture content occurs up to about 200 °C (dehydration stage), and the actual decomposition (degradation of hemicellulose, cellulose, and certain lignin) occurs between 200-600 °C. The condensation, characterized by the decomposition of the lignin component of the feedstock, happens at temperatures >600 °C. The DTG graph of the raw biomass (Fig. 6c) showed 2 distinct peaks at 320 °C and 500 °C, matching decomposition and condensation temperatures. TG height of the raw biomass is higher than the pyrolysis char (Fig. 6b), indicating that the raw biomass undergoes significant degradation compared to the pyrolysis chars under the same condition. In addition, it further revealed that pyrolysis treatment results in the generation of biochar and better thermal stability (Ibitoye et al. 2022; Ibitoye et al. 2021b).

The DTG curves of the pyrolysis chars (Fig. 6d) show no noticeable mass loss at the dehydration stage until the attainment of 400 °C, which implies that the dehydration of the biochar had already occurred throughout the pyrolysis process. The breakdown of the biochar occurs between 500 and 700 °C. This involves additional and significant mass loss of the cellulose and hemicellulose portion of the biochar. The condensation occurs between 700-800 °C, and is characterized by the decomposition of cellulose and lignin components from

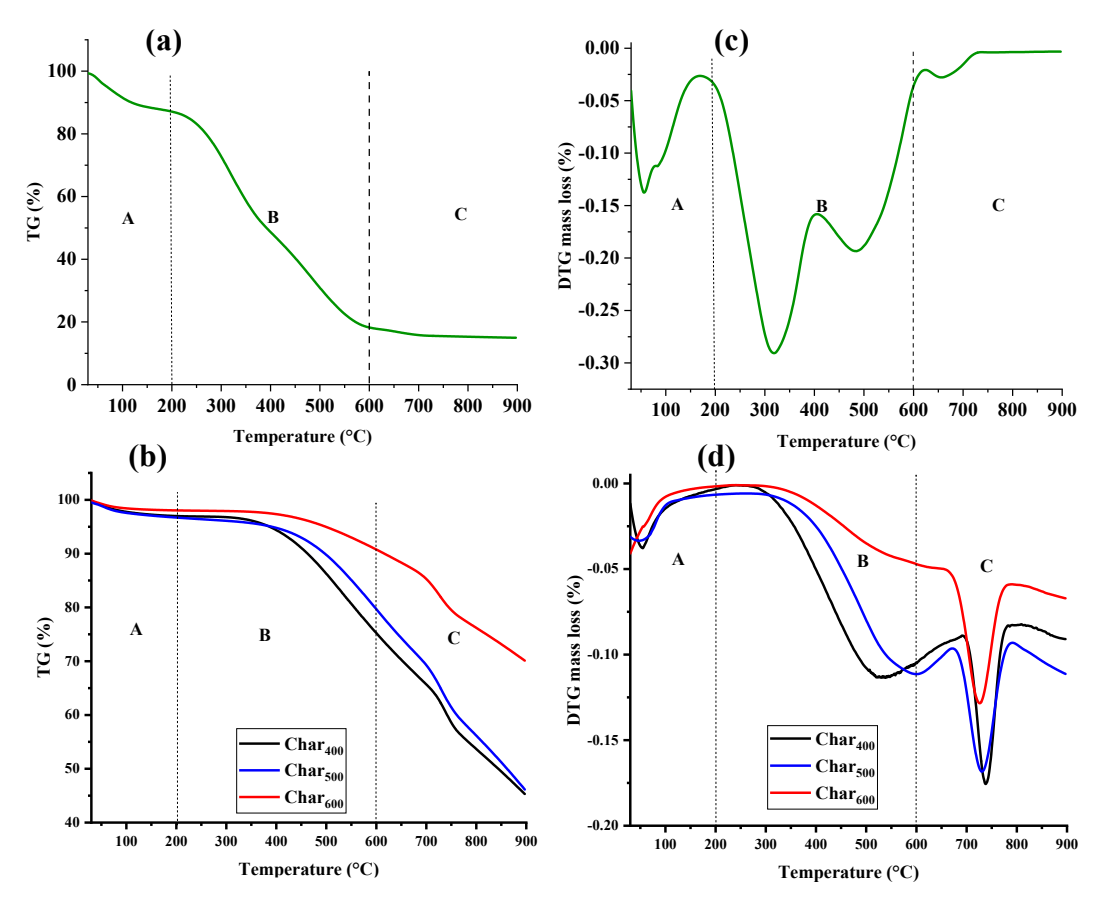


Fig. 6 Plot of TG (a) raw biomass, (b) char, and DTG (c) raw biomass, (d) char

the biochar. Lignin is the most stable constituent of the biochar and requires a temperature >700 °C to decompose.

The TG and DTG curves revealed that pyrolysis enhances the thermal stability of biomass. This finding is noteworthy as the biochar produced from MTL compares favorably with coal, and it is suitable for high-temperature applications, such as a feedstock for power plants that generate electricity.

3.6. Degree of pyrolysis and fuel ratio

Fuel ratio and degree of pyrolysis are crucial variables that impact the effectiveness and suitability of biochar as an alternative to conventional carbon in iron and steel production. The degree of pyrolysis is an indication of the carbon content of the produced fuels, while the fuel ratio signifies a greater percentage of fixed carbon compared to volatile matter in the produced fuels. Appropriate fuel ratio and higher degree of (lower dr value) enhanced the combustion characteristics, energy density, and ecological performance of fuels. Fig. 7 shows the variation of fuel ratio and degree of pyrolysis with temperature. It was observed that the degree of pyrolysis decreases from 0.21 to 0.07 with temperature, while the fuel ratio increases (from 4.8 to 14.78) as the pyrolysis temperature increases. The observed trend was due to the release of VM from the raw biomass, which led to an increase in FC while reducing VM. The findings showed a noticeable increase in fuel ratio coupled with a decrease in the degree of pyrolysis. The highest and lowest fuel ratios correspond to the chars produced at 400, and 600 °C, respectively. This trend aligns with the research carried out by Ibitoye et al. (2021b), utilizing corncob as feedstock, which reported a corresponding augmentation in fuel ratio with rising process temperature. Further, Wojtacha-Rychter and Smoliński (2019) reported a fuel

ratio of about 1.68 for bituminous coal, which is lower than the value obtained in this study. However, anthracite displayed an exceptional fuel ratio of about 23.255 (Kieush *et al.*, 2022).

This could be linked to the higher FC, lower VM, and lower impurities properties of anthracite. Small fuel ratio values suggest that the fuel's combustion is characterized by a larger flame, rapid burnout, and minimal char production. The pyrolysis-based thermochemical treatment produced a fuel ratio conducive to sustained and steady combustion, enhancing its suitability for energy applications. Likewise, a lower pyrolysis

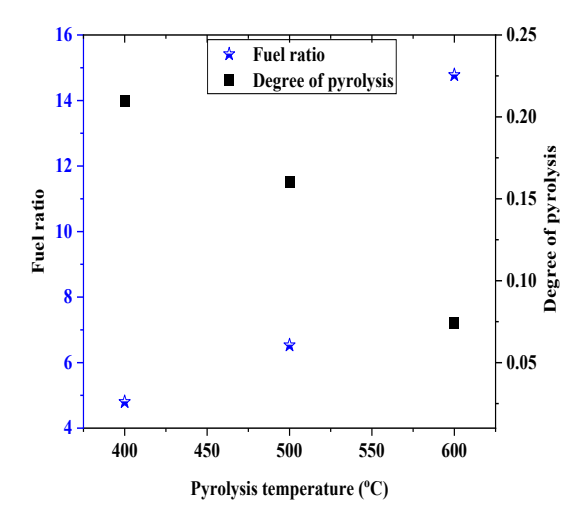


Fig. 7 Variation of the degree of pyrolysis and fuel ratio with temperature

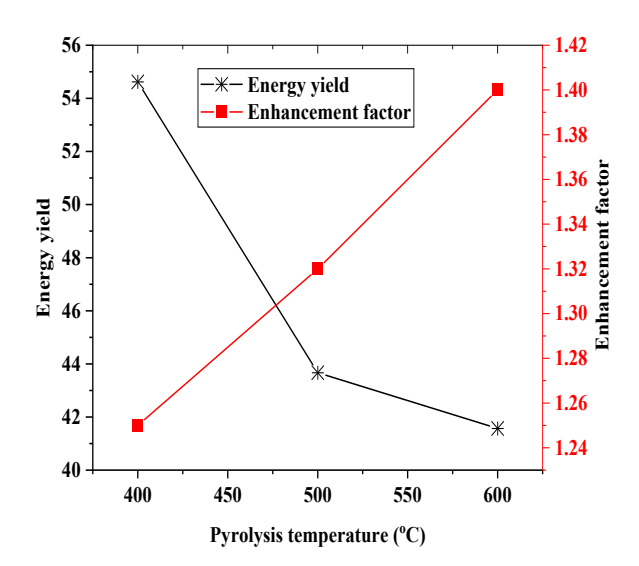


Fig. 8 Variation of energy yield and enhancement factor with temperature

intensity correlated with fuel exhibiting stable combustion characteristics.

Analysis of the results revealed that $Char_{600}$ demonstrates properties suitable for energy applications, such as an alternative to coal and coke in iron and steel making. This can be linked to its higher fuel ratio and lower degree of pyrolysis values, indicating it as a fuel with steady and prolonged combustion, appropriate for energy applications.

3.7. Energy yield and enhancement factor

The importance of the enhancement factor and energy yield of the produced biochar lies in efficiency, cost-effectiveness, and sustainability. A high-energy yield shows that a larger percentage of the feedstock is retained in the biochar, hence making the biochar an efficient solid fuel. Higher energy yield can minimize costs and dependency on fossil fuels, which enhances the eco-friendly production process.

Notably, the highest enhancement factor and energy yield of 1.40 and 55.24, respectively, were recorded at 600 °C, while the corresponding lowest values of 1.24 and 42.43 were obtained at 400 °C (Fig.8). Enhancement factor values positively correlated with an increase in pyrolysis temperatures. In contrast, energy yields demonstrate an inverse relationship with temperature, diminishing with an increase in pyrolysis temperatures. This is explained by the fact that energy yield depends on solid yield (mass yield), which decreases with temperature (Fig. 8). As shown in Fig. 5, the HHV of the pyrolysis products also followed the patterns observed in the enhancement factor values shown in Fig. 8. The Char₆₀₀ displayed the highest enhancement factor value. This implies

that $Char_{600}$ will display efficient combustion characteristics (compared to $Char_{400}$ and $Char_{500)}$, which is essential for high energy use for metallurgical processes. It also suggests that $Char_{600}$ is a better alternative to conventional carbon sources such as coal in iron and steel production. The values suggest that the biochars generated are suitable for various energy generation applications, including co-combustion in power plants and briquetting for both domestic and industrial use.

3.8. Fuel and flow properties

Hausner ratios (HR) and Carr Compressibility Index (CCI) provide insight into the flowability, handling, storage, transportation, and combustion characteristics of solid fuels. Biochar with good HR can enhance the effectiveness of material handling and encourage uniform and consistent combustion, which improves the overall operational efficiency during application. CCI measures the densification properties, which are crucial for uniform combustion and efficiency of solid fuels. According to Lumay *et al.* (2012) and Szalay, Kelemen, and Pintye-Hódi (2015), biochar with an HR between 1.19 and 1.25 exhibits fair flowability, while an HR range of 1.12 to 1.18 indicates good flow properties. Similarly, a CCI between 11-15 corresponds to good flow behavior, 16-20 indicates fair flow, and 21-25 represents passable flowability.

Table 3 presents the HR, CCI, bulk density, and tapped density of the produced biochar. It is evident that with increasing process temperature, HR and CCI values decrease from 1.29 to 1.14 and from 22.48 to 12.59, respectively. This shows that the biochar generated at higher temperatures (Char₆₀₀) exhibits good flow and flow and compressibility (density) properties (Tannous *et al.*, 2013). All the biochars generated in this study displayed excellent compressibility properties. This suggests enhanced fluidity property, encouraging densification such as pelletizing or briquetting from the produced biochar. It also indicated that they will be easier to store and transport. Furthermore, it also suggests that the chars will generate less dust and be less prone to clogging in conveyors and hoppers, thus making material handling more efficient and cost-effective.

3.9. Morphological characteristics

The porosity, elemental, and surface characteristics of the raw biomass and biochar were revealed by the SEM image. These properties influence the reactivity, absorption, and energy properties of the biomass and pyrolysis char. Analysis of the SEM results revealed that the temperature meaningfully impacts the morphological properties of the feedstock. The pore formation and porosity increase with temperature (Hadey *et al.*, 2022). The comparison between the change in surface morphology of the biochar and raw biomass with temperature is illustrated in Fig. 9. The raw biomass (Fig. 9a) displays a rough surface morphological feature with flaky micro-particles, suggesting likely cavities. The SEM image showed that the biomass feedstock becomes softer, melts, and rages into a mass

Table 3

Sample	Bulk density (g/mL)	Tapped density (g/mL)	CCI (%)	Hausner ratio
Char ₄₀₀	0.232	0.30	22.48	1.29
Char ₅₀₀	0.219	0.28	21.49	1.27
Char ₆₀₀	0.201	0.23	12.59	1.14

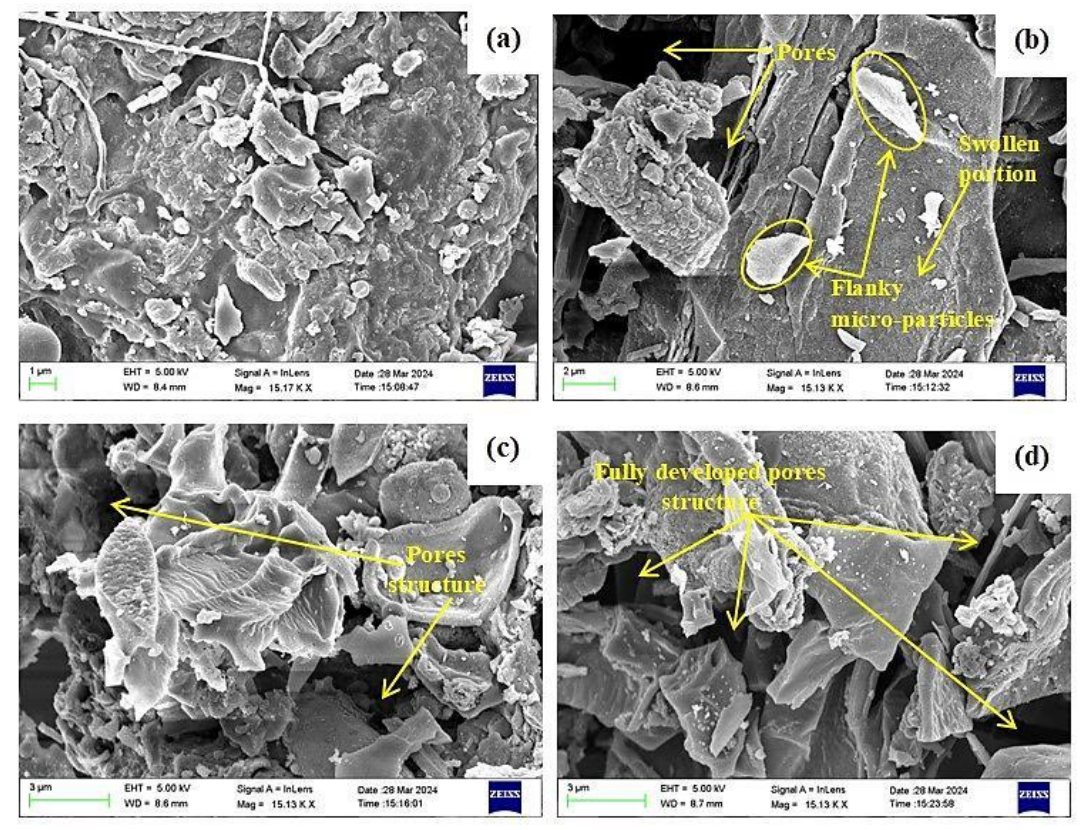


Fig. 9 SEM image of the (a) raw biomass, (b) Char₄₀₀, (c) Char₅₀₀, and (d) Char₆₀₀

of puffy and crumbling micro-particles (Fig. 9b) due to the emission of VM within the biomass (Zhao et al., 2017). Significant transformations in microstructure are evident when the SEM images of raw biomass (Fig. 9a) and biochar are compared. With increasing temperatures, more volatile matters are released, causing the swollen and flaky particles on the surface of (Fig. 9b) to burst after cooling, resulting in a porous morphology. Char500 exhibits percentages of the skeletal configuration appearing brittle due to the degradation of more components, and fracture phenomena are observed within the pore structure for Char₆₀₀ (Hadey et al., 2022).

The observed trend aligns with the results of Nugraha et al. (2022), who reported increased pore structure formation with higher pyrolysis temperatures. This increase in porosity is desirable for various applications, such as serving as a reducing agent in metallurgical processes, soil remediation, and water treatment.

Previous studies have noted the development of a wellordered porous structure at high pyrolysis temperatures;

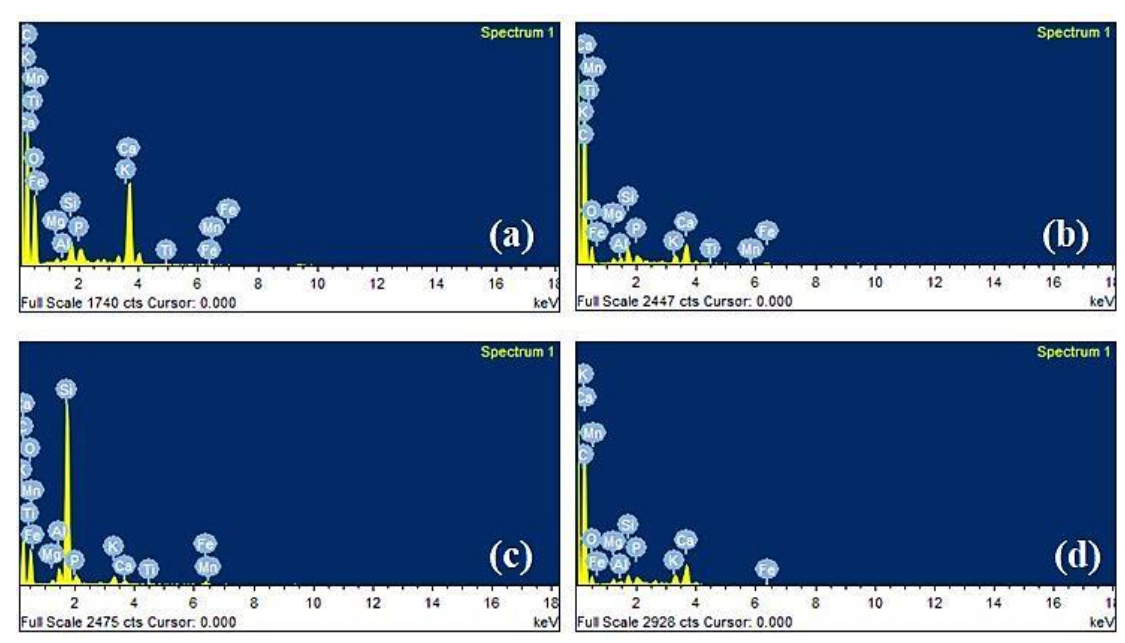


Fig. 10 EDX plot of (a) raw biomass, (b) Char₄₀₀, (c) Char₅₀₀, and (d) Char₆₀₀

Table 4

Elemental composition of the raw biomass and biochar	I UDIC I				
	Elemental composition	of the raw	biomass	and	biochar

Element (K)	Raw biomass (wt.%)	Char ₄₀₀ (wt.%)	Char ₅₀₀ (wt.%)	Char ₆₀₀ (wt.%)
С	45.70	59.48	68.34	71.75
0	40.68	31.26	21.44	16.83
Mg	0.39	0.42	0.63	0.75
Al	0.03	1.31	0.48	0.30
Si	1.37	2.21	1.68	1.33
P	0.34	0.51	0.34	0.46
K	0.81	1.53	1.70	2.35
Ca	10.47	2.31	4.45	5.05
Ti	0.04	0.27	0.16	0.00
Mn	0.05	0.11	0.15	0.19
Fe	0.11	0.59	0.62	0.99
Total	100	100	100	100

however, the biochar generated in this study does not exhibit such orderliness (Boulemkahel et al., 2021; Hadey et al., 2022; Ighalo & Adeniyi, 2020). This disparity could stem from differences in the feedstock and processing methods used for each study. Additionally, the disagreement in biochar structure may result from the mixture of various tree leaves used in the current study, as opposed to previous studies that utilized a single biomass as feedstock.

Elemental analysis (Fig. 10 and Table 4) revealed that char₆₀₀ exhibited the highest carbon and lowest oxygen content. which agrees with the findings presented in Table 2. The liberation of moisture and CO2 initiates dehydroxylation and decarboxylation reactions, likely leading to a decline in oxygen levels. Simultaneously, oxygen release may also manifest as CO and other oxygen-bearing gases (Patil et al., 2023). The high carbon content underscores the potential of biochar for energy applications. The property benefits solid fuel utilization, including serving as a substitute for coal in blast furnaces (BF) and injectant in BF tuyeres. An investigation conducted on the utilization of biochar as an injectant in BF revealed that biochar increases BF burnout compared to coals and increases operating costs (Gil et al., 2015; Pohlmann et al., 2016). Furthermore, biochar can be mixed with coal in power plants for energy production and alternative to Coke Breeze in iron and steel production (Khanna et al., 2019). Previous research has revealed that using a biochar blend with coke breeze enhanced sintering speed. However, a reduction in sinter yields and productivity was reported at a higher blending ratio (El-Hussiny et al., 2015; Mousa et al., 2015). Also, using biochar as a coke

breeze reduces the bulk density of the sinter, encourages quick combustion, and results in a thinner sintering and combustion region in BF.

The presence of Mg, P, Al, and K revealed the biochar potential for agricultural applications, such as soil remediation, to enhance crop production (Danesh et al., 2023; Zhang et al., 2012). P is essential for plant photosynthesis and root growth, while K controls water uptake and stress resistance. Al enhances crop growth, particularly in acidic soils. Mg plays a crucial role in plant chlorophyll generation, an essential plant component for photosynthesis. The availability of the element in soil significantly impacts plant growth and productivity (Osman et al., 2022; Tan, 2023).

3.10. Pore-size distribution and BET surface area

The BET surface area, pore volume, and pore radius are vital parameters that influence the reactivity, adsorption capacity, catalytic properties, combustion kinetics, and heat transfer properties of the produced solid fuels. The results of the morphological characteristics of the produced chars are displayed in Fig. 11. The results showed that the BET surface area, pore volume, and pore radius of the produced chars increase with temperature. The highest surface area and pore volume of 17.36 m²/g and 0.058 cc/g, respectively, were recorded for Char₆₀₀ samples, while the least surface area (3.45 m²/g) and pore volume (0.029 cc/g) were obtained from the Char₄₀₀ samples. Char₆₀₀ displayed a better surface area property of 17.36 m²/g compared to traditional carbon sources

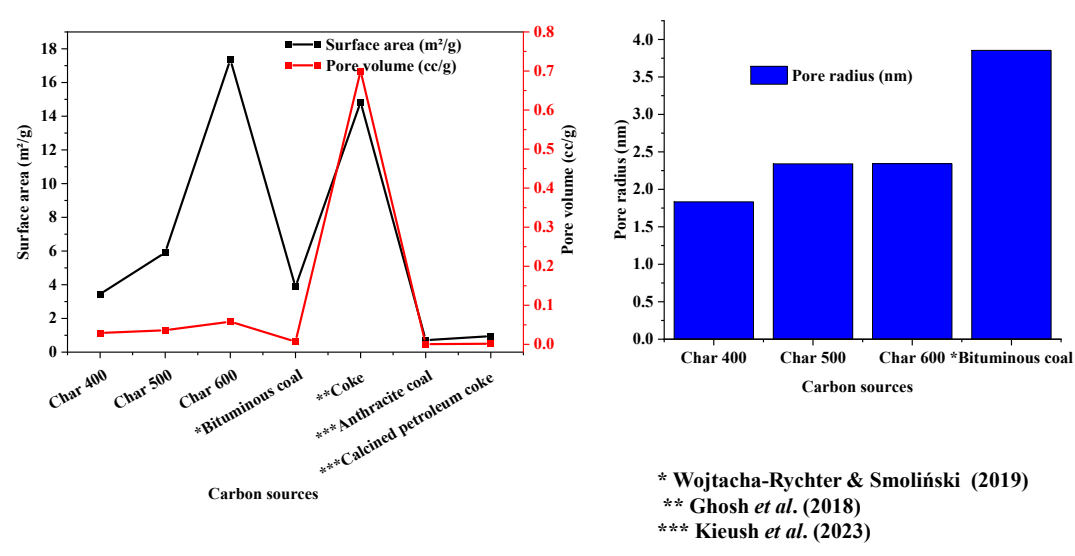


Fig. 11 BET surface area and pore-size distribution of the produced biochar compared to other carbon sources

such as coke (14.84 m²/g), anthracite coal (0.71 m²/g), bituminous coal (3.88 m²/g), and calcined petroleum coke (0.95 m²/g) (Ghosh et al., 2018; Kieush et al., 2023; Wojtacha-Rychter & Smoliński, 2019). A similar trend was also observed with the pore volume and pore radius, except for coke, which had the highest pore volume of 0.700 cc/g, and bituminous coal, which had the highest pore radius of 3.855 nm. The increase in surface area can be associated with thermal treatment via pyrolysis, which transforms the surface properties of char by increasing its surface area and reducing its oxygen and volatile content (Mendonça et al., 2017). It can be deduced from Fig. 11 that the chars generated from MTL, especially the Char₆₀₀, can substitute coal and coke in iron and steel production, and this deduction is in line with the results of Kieush et al. (2022) and Safarian (2023), who reported that biochar can replace coal and coke and iron and steel production. Leng et al. (2021) in their report opined that outstanding surface area and pore volume can increase reactivity during iron and steel production by providing sufficient sites for chemical reactions. Furthermore, the larger surface area enhances the char's capability to absorb impurities and its catalytic characteristics, which are beneficial in various metallurgical applications (Kieush et al., 2022; Safarian, 2023). Higher pore volume encourages efficient gas diffusion, improving combustion efficiency.

The BET surface area of biochars produced from MTL (3.45–17.36 m²/g) is considerably higher than biochars derived from mahogany leaves by Putri, Sarifuddin, and Bintang (2023), which recorded 5.47 m²/g at 409 °C. Similarly, it surpasses the biochar from poplar leaves, which exhibited surface areas in the range of 0.82-2.6 m²/g across 400-600 °C (Qiu et al., 2023). The increased BET surface area observed in this study aligns well with trends reported by Babu et al. (2024), who also noted that higher pyrolysis temperatures promote volatile release and pore development in biochars. Morphologically, the SEM images of Char₆₀₀ revealed well-developed porous networks and fractured surfaces, attributed to volatile matter release and structural collapse during high-temperature treatment. In contrast, the mahogany leaves' biochar produced at 409 °C retained relatively smoother surfaces with fewer pores. The MTL used in this study, due to their diversity, likely contributed to a more robust microstructural evolution compared to single-type biomass systems.

3.11.Product yield

As per Fig. 12, the results show that bio-oil (26.13-39.95%) and syngas production (30.33-39.38%) increase with temperature. On the other hand, the char production dropped from 43.66-29.67% as the pyrolysis temperature increased. Elevated temperatures are essential for increasing the yields of gas and oil from pyrolysis because they increase the rate at which chemical bonds in biomass are broken. Increased thermal energy makes it easier for biomass to break down, which causes more volatiles to be released (Ibitoye et al. 2021b). A more significant percentage of biomass is transformed into gas and oil at higher temperatures. The synergistic effects of the simultaneous secondary degradation of biochar generated throughout the primary degradation phase and the increased primary decomposition of biomass are responsible for this occurrence (Selvarajoo & Oochit, 2020). Thus, the oil and gas generation, while the char decreases as the pyrolysis temperature rises.

The product yield observed in this study aligned with trends reported in recent literature. This behavior aligns well with the findings of Qiu *et al.* (2023), where poplar leaves showed a biochar yield decrease from 33.8% to 24.2%, accompanied by an increase in bio-oil and syngas yields. Similarly, Babu *et al.*

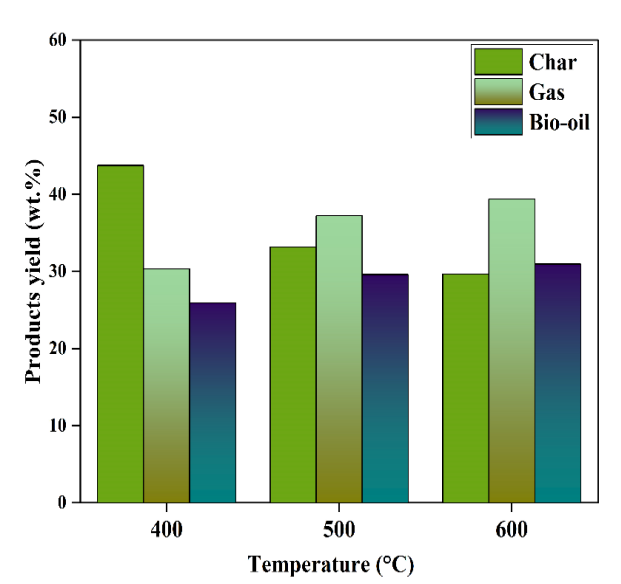


Fig. 12 Variation of pyrolysis product yield with temperature

(2024) reported an increase in volatile products and a corresponding drop in solid residue when mixed wood and coconut husk were pyrolyzed at higher temperatures. Pyrolyzed Mahogany leaves produced about 25% char at 409 °C, comparable to the results of the study at 400 °C (Putri et al., 2023). Further, Durango Padilla et al. (2024) noted a similar decline in mass yield across coconut shell and corncob biomass as pyrolysis temperatures were raised, attributing it to enhanced thermal degradation of volatiles. These trends are scientifically justified as elevated temperatures promote secondary cracking reactions, increased volatile release, and decomposition of oxygen-containing functional groups, thereby reducing solid yield and enriching liquid and gas fractions (Ibitoye et al. 2021b; Selvarajoo and Oochit 2020). The yield distribution in the present study is well-supported by the broader biomass literature, strengthening the reliability applicability of the findings.

4. Conclusion and recommendation

4.1. Conclusion

This study examined how pyrolysis process parameters affected the energetic and physicochemical characteristics of biochars and the production of hydrogen from MTL in a fixed-bed reactor on a pilot-scale. The physicochemical properties of the biochar were evaluated and determined to be superior to those of the feedstock biomass. By raising the pyrolysis temperature, the HHV of biochars was enhanced (20.78-23.32 MJ/kg), which led to an increase in the energy yield.

The degree of pyrolysis and fuel ratio values varied between 0.46-0.88 and 0.18-1.29, respectively. Notably, the lowest and highest enhancement factor of 1.24 and 1.40 was recorded at 400 and 600 °C, respectively. Pyrolysis enhances the thermal stability of biomass, with improvements correlating with higher pyrolysis temperatures.

The higher BET surface area of the chars, particularly Char₆₀₀ (17.36 m²/g), enhances reactivity and adsorption capacity, improving combustion efficiency and impurity removal in metallurgical processes. The larger surface area and higher pore volume facilitate efficient gas diffusion and stable combustion, leading to more consistent and efficient fuel usage. Char600's surface characteristics enhance its catalytic

properties, benefiting various metallurgical reactions and potentially increasing process efficiency. Utilizing the char generated from MTL can reduce reliance on the iron and steel industries on non-renewable resources, lowering their carbon footprint, and supporting waste management by turning waste leaves into valuable biochar.

The pyrolysis liquid yield demonstrated that MTL may be used to produce biodiesel for fuel applications; however, more research must be done on the fuel's characteristics. This research encourages the development of more sustainable energy options from biomass waste, such as tree leaves. This could lessen the dependence on fossil fuels and the adverse effects that dumping and burning tree leaves have on the environment.

The pyrolyzed leaf biomass produces biochar with fixed carbon, porosity, and surface area comparable to coal and superior to several agro-residues, supporting its use in energy and metallurgical applications.

4.2. Recommendation for future studies

The applicability of mixed tree leaves biochar in industrial processes such as blast furnace injection or co-firing should be validated through pilot trials or simulations. Future studies should incorporate direct elemental analysis (CHNOS) to quantify nitrogen and sulfur contents, which are essential for evaluating NOx and SOx emissions. Detailed syngas composition analysis and characterization of pyrolysis oil properties are also recommended to assess their energy potential and upgrade options. Techno-economic assessments and life cycle analysis are needed to evaluate the scalability and environmental impacts of converting mixed tree leaves into high-value biochar and bioenergy products.

Acknowledgments

The authors thank CSIR-CMERI, Durgapur, for providing research facilities and also acknowledge the support of the Director

Author contributions

S.E.I. and M.A.: Conceptualization, methodology, validation; O.A.O. and M.A.: formal analysis; S.E.I: writing—original draft; C.L., R.M.M., T-C.J., and E.T.A.: supervision, writing—review and editing. All authors read and approved the final manuscript.

Funding statement

The authors appreciate CSIR, New Delhi, for providing financial support through the CSIR-SRF(GATE) fellowship (File No: 31/GATE/19(73)/2021-EMR-1).

Competing Interest

The authors have no non-financial or financial interest to disclose.

References

- Abdullah, N., Mohd Taib, R., Mohamad Aziz, N. S., Omar, M. R., & Md Disa, N. (2023). Banana pseudo-stem biochar derived from slow and fast pyrolysis process. *Heliyon*, *9*(1), e12940. https://doi.org/10.1016/j.heliyon.2023.e12940
- Adekunle, A. S., Ibitoye, S. E., Omoniyi, P. O., Jilantikiri, L. J., Yahaya, T., Mohammad, B. G., & Olusegun, H. D. (2019). *Production and Testing of Biogas Using Cow Dung, Jatropha and Iron Filins.* 4(3), 143–148. https://doi.org/10.12162/jbb.v4i3.002
- Adelawon, B. O., Latinwo, G. K., Eboibi, B. E., Agbede, O. O., Agarry, S.

- E., Latinwo, G. K., Eboibi, B. E., & Agbede, O. O. (2021). Comparison of the slow, fast, and flash pyrolysis of recycled maize-cob biomass waste, box-benhken process optimization and characterization studies for the thermal fast pyrolysis production of bio-energy. *Chemical Engineering Communications*, *0*(0), 1–31. https://doi.org/10.1080/00986445.2021.1957851
- Adeniyi, A. G., Iwuozor, K. O., Adeleke, J., Emenike, E. C., Micheal, K. T., & Ighalo, J. O. (2023). Production and characterization of neem leaves biochar: Effect of two different retort carbonization systems. *Bioresource Technology Reports*, 24(June), 101597. https://doi.org/10.1016/j.biteb.2023.101597
- Adeniyi, A. G., Iwuozor, K. O., Emenike, E. C., Amoloye, M. A., Adeleke, J. A., Omonayin, E. O., Bamigbola, J. O., Ojo, H. T., & Ezzat, A. O. (2024). Leaf-based biochar: A review of thermochemical conversion techniques and properties. *Journal of Analytical and Applied Pyrolysis*, 177(January), 106352. https://doi.org/10.1016/j.jaap.2024.106352
- Ahmed, A., Abu Bakar, M. S., Hamdani, R., Park, Y. K., Lam, S. S., Sukri, R. S., Hussain, M., Majeed, K., Phusunti, N., Jamil, F., & Aslam, M. (2020). Valorization of underutilized waste biomass from invasive species to produce biochar for energy and other value-added applications. *Environmental Research*, 186(February), 109596. https://doi.org/10.1016/j.envres.2020.109596
- Al Hosni, S., Domini, M., Vahidzadeh, R., & Bertanza, G. (2024).

 Potential and Environmental Benefits of Biochar Utilization for Coal/Coke Substitution in the Steel Industry. *Energies*, 17(11). https://doi.org/10.3390/en17112759
- Alam, M., Sarkar, I., Chanda, N., Ghosh, S., & Loha, C. (2024). Enhancing syngas production and hydrogen content in syngas from catalytic slow pyrolysis of biomass in a pilot-scale fixed-bed reactor. *Biomass Conversion and Biorefinery*, 1–13. https://doi.org/10.1007/s13399-024-05453-0
- Antonangelo, J. A., Sun, X., & Eufrade-Junior, H. de J. (2025). Biochar impact on soil health and tree-based crops: a review. *Biochar*, 7(1). https://doi.org/10.1007/s42773-025-00450-6
- Ariyanti, D., Widiasa, I.N., Widiyanti, M., Lesdantina, D., Gao, W. (2023).

 Agricultural waste-based magnetic biochar produced via hydrothermal route for petroleum spills adsorption. *International Journal of Renewable Energy Development*, 12 (3), pp. 499 507. https://doi.org/10.14710/ijred.2023.52180
- Asadi Zeidabadi, Z., Bakhtiari, S., Abbaslou, H., & Ghanizadeh, A. R. (2018). Synthesis, characterization and evaluation of biochar from agricultural waste biomass for use in building materials. Construction and Building Materials, 181, 301–308. https://doi.org/10.1016/j.conbuildmat.2018.05.271
- ASTM D3175-11. (2013). Standard Test Method of Volatile Matter in Biomass. ASTM International, West Conshohocken, PA. https://www.astm.org
- ASTM E1755-01. (2015). Standard Test Method for ash in Biomass. ASTM International, West Conshohocken, PA. https://www.astm.org
- ASTME177-19. (2019). Standard Practice for Use of the Terms Precision and Bias in ASTM Test Methods. ASTM International, West Conshohocken. PA.
- Babu, K. K. B. S., Nataraj, M., Tayappa, M., Vyas, Y., Mishra, R. K., & Acharya, B. (2024). Production of biochar from waste biomass using slow pyrolysis: Studies of the effect of pyrolysis temperature and holding time on biochar yield and properties. *Materials Science for Energy Technologies*, 7(November 2023), 318–334. https://doi.org/10.1016/j.mset.2024.05.002
- Basu, P. (2010). Biomass Characteristics. In *Biomass Gasification Design Handbook* (First Edition). © 2010 Elsevier Inc. https://doi.org/10.1016/b978-0-12-374988-8.00002-7
- Boulemkahel, S., Betoret, E., Benatallah, L., & Rosell, C. M. (2021). Effect of low-pressure homogenization on the physico-chemical and functional properties of rice flour. *Food Hydrocolloids*, *112*, 106373. https://doi.org/10.1016/j.foodhyd.2020.106373
- Christwardana M., Suedy S.W.A., Harmoko U., Malika A., Dayanti D. (2025). Carbonization and aromaticity-driven electron transfer in hydrochars from tropical woods as electrochemical cell electrode for energy conversion and storage. *Bioresource Technology Reports*, 30, art. no. 102107. https://doi.org/10.1016/j.biteb.2025.102107
- Cormos, C. (2023). Green hydrogen production from decarbonized biomass gasification: An integrated techno-economic and environmental analysis. *Energy*, 270(February), 126926.

https://doi.org/10.1016/j.energy.2023.126926

- Danesh, P., Niaparast, P., Ghorbannezhad, P., & Ali, I. (2023). Biochar Production: Recent Developments, Applications, and challenges. *Fuel*, 337(November 2022), 126889. https://doi.org/10.1016/j.fuel.2022.126889
- De Bhowmick, G., Sarmah, A. K., & Sen, R. (2018). Production and characterization of a value-added biochar mix using seaweed, rice husk and pine sawdust: A parametric study. *Journal of Cleaner Production*, 200, 641–656. https://doi.org/10.1016/j.jclepro.2018.08.002
- Durango Padilla, E. R., Hansted, F. A. S., Luna, C. M. R., de Campos, C. I., & Yamaji, F. M. (2024). Biochar derived from agricultural waste and its application as energy source in blast furnace. Renewable Energy, 220, 119688. https://doi.org/10.1016/j.renene.2023.119688
- El-Hussiny, N. A., Khalifa, A. A., El-midany, A. A., Ahmed, A. A., & Shalabi, M. E. H. (2015). Effect of replacement coke breeze by charcoal on technical operation of iron ore sintering. *International Journal of Scientific & Engineering Research*, 6(2). https://www.ijser.org/paper/Effect-of-replacement-coke-breeze-by-charcoal-on-technical-operation.html
- Fraia, S. Di, Shah, M., & Vanoli, L. (2023). A biomass-based polygeneration system for a historical building: A technoeconomic and environmental analysis. *Energy Conversion and Management*, 291(April), 117336. https://doi.org/10.1016/j.enconman.2023.117336
- Gabbar, H. A., & Aboughaly, M. (2021). Conceptual process design, energy and economic analysis of solid waste to hydrocarbon fuels via thermochemical processes. *Processes*, 9(12). https://doi.org/10.3390/pr9122149
- Ghosh, B., Sahoo, B. K., Chakraborty, B., Manjhi, K. K., Das, S. K., Sahu, J. N., & Varma, A. K. (2018). Influence of coke structure on coke quality using image analysis method. *International Journal of Coal Science and Technology*, 5(4), 473–485. https://doi.org/10.1007/s40789-018-0227-0
- Gil, M. V., García, R., Pevida, C., & Rubiera, F. (2015). Grindability and combustion behavior of coal and torrefied biomass blends. Bioresource Technology, 191, 205–212. https://doi.org/10.1016/j.biortech.2015.04.117
- Gupta, A., Siddiqui, H., Rathi, S., & Mahajani, S. (2021). Intra-pellet transport limitations in the pyrolysis of raintree leaves litter. *Energy*, 216, 119267. https://doi.org/10.1016/j.energy.2020.119267
- Gupta, S., Kishore, N., Ahmed, G., & Kumari, K. (2024). Catalytic copyrolysis of leaves of Polyalthia longifolia, woods of Delonix regia and polypropylene grocery bags using zeolite Y-hydrogen catalyst. *Biomass Conversion and Biorefinery*, 14(14), 15649–15659. https://doi.org/10.1007/s13399-022-03731-3
- Hadey, C., Allouch, M., Alami, M., Boukhlifi, F., & Loulidi, I. (2022). Preparation and Characterization of Biochars Obtained from Biomasses for Combustible Briquette Applications. Scientific World Journal, 2022, 1–13. https://doi.org/10.1155/2022/2554475
- Haniif P., Dewi S.F., Hadiyanto H., Widya F.(2024). Catalytic Pyrolysis of Biomass Waste Mixture over Activated Carbon and Zeolite Catalyst for the Production Bio Oil. Key Engineering Materials, 978,107 - 117, https://doi.org/10.4028/p-9IGsFm
- Huang, X., Cao, J. P., Zhao, X. Y., Wang, J. X., Fan, X., Zhao, Y. P., & Wei, X. Y. (2016). Pyrolysis kinetics of soybean straw using thermogravimetric analysis. Fuel, 169, 93–98. https://doi.org/10.1016/j.fuel.2015.12.011
- Ibitoye, S. E., Ajimotokan, H. A., Adeleke, A. A., & Loha, C. (2023). Effect of densification process parameters on the physico-mechanical properties of composite briquettes of corncob and rice husk. *Materials Today: Proceedings, June 2023*, 1–7. https://doi.org/10.1016/j.matpr.2023.08.253
- Ibitoye, S. E., Jen, T. C., Mahamood, R. M., & Akinlabi, E. T. (2021a). Densification of agro-residues for sustainable energy generation: an overview. *Bioresources and Bioprocessing*, 8(75), 1–19. https://doi.org/10.1186/s40643-021-00427-w
- Ibitoye, S. E., Jen, T., Mahamood, R. M., & Akinlabi, E. T. (2021b). Generation of Sustainable Energy from Agro-Residues through Thermal Pretreatment for Developing Nations: A Review. Advanced Energy and Sustainability Research, 2100107, 1–15. https://doi.org/10.1002/aesr.202100107

- Ibitoye, S. E., Jen, T., Mahamood, R. M., & Akinlabi, E. T. (2021c). Improving the Combustion Properties of Corncob Biomass via Torrefaction for Solid Fuel Applications. *Journal of Composite Science*, 5(10), 1–15. https://doi.org/10.3390/jcs5100260
- Ibitoye, S. E., Loha, C., Mahamood, R. M., Jen, T., Alam, M., & Sarkar, I. (2024). An overview of biochar production techniques and application in iron and steel industries. *Bioresources and Bioprocessing*, 11(65), 1–35. https://doi.org/10.1186/s40643-024-00779-z (2024)
- Ibitoye, S. E., Mahamood, R. M., Jen, T.-C., & Akinlabi, E. T. (2022). Combustion, Physical, and Mechanical Characterization of Composites Fuel Briquettes from Carbonized Banana Stalk and Corncob. *International Journal of Renewable Energy Development*, 11(2), 435–447. https://doi.org/10.14710/ijred.2022.41290
- Ighalo, J. O., & Adeniyi, A. G. (2020). A mini-review of the morphological properties of biosorbents derived from plant leaves. SN Applied Sciences, 2(3), 1–16. https://doi.org/10.1007/s42452-020-2335-x
- Irfan, M., Chen, Q., Yue, Y., Pang, R., Lin, Q., Zhao, X., & Chen, H. (2016). Co-production of biochar, bio-oil and syngas from halophyte grass (Achnatherum splendens L.) under three different pyrolysis temperatures. *Bioresource Technology*, 211, 457–463. https://doi.org/10.1016/j.biortech.2016.03.077
- Khanna, R., Li, K., Wang, Z., Sun, M., Zhang, J., & Mukherjee, P. S. (2019). Biochars in iron and steel industries. *Char and Carbon from Biomass*, 2017. https://doi.org/10.1016/B978-0-12-814893-8.00011-0
- Khater, E. S., Bahnasawy, A., Hamouda, R., Sabahy, A., Abbas, W., & Morsy, O. M. (2024). Biochar production under different pyrolysis temperatures with different types of agricultural wastes. Scientific Reports, 14(1), 1–8. https://doi.org/10.1038/s41598-024-52336-5
- Kieush, L., Rieger, J., Schenk, J., Brondi, C., Rovelli, D., Echterhof, T., Cirilli, F., Thaler, C., Jaeger, N., Snaet, D., Peters, K., & Colla, V. (2022). A Comprehensive Review of Secondary Carbon Bio-Carriers for Application in Metallurgical Processes: Utilization of Torrefied Biomass in Steel Production. *Metals*, 12(2005), 1–38. https://doi.org/10.3390/met12122005
- Kieush, L., Schenk, J., Koveria, A., Hrubiak, A., Hopfinger, H., & Zheng, H. (2023). Evaluation of Slag Foaming Behavior Using Renewable Carbon Sources in Electric Arc Furnace-Based Steel Production. *Energies*, 13(722), 1–16. https://doi.org/10.3390/en16124673
- Kongto, P., Palamanit, A., Chaiprapat, S., & Tippayawong, N. (2021). Enhancing the fuel properties of rubberwood biomass by moving bed torrefaction process for further applications. *Renewable Energy*, *RENE* 14903, 1–30. https://doi.org/10.1016/j.renene.2021.02.012
- Lahiri, A., Daniel, S., Kanthapazham, R., Vanaraj, R., Thambidurai, A., & Sophie, L. (2023). A critical review on food waste management for the production of materials and biofuel. *Journal of Hazardous Materials Advances*, *10*(February), 100266. https://doi.org/10.1016/j.hazadv.2023.100266
- Leng, L., Xiong, Q., Yang, L., Li, H., Zhou, Y., Zhang, W., Jiang, S., Li, H., & Huang, H. (2021). An overview on engineering the surface area and porosity of biochar. Science of the Total Environment, 763, 144204. https://doi.org/10.1016/j.scitotenv.2020.144204
- Loo, S. van, & Koppejan, J. (2008). *The Handbook of Biomass Combustion and Co-firin* (S. van Loo & J. Koppejan (eds.); Issue 112). Earthscan.
- Lumay, G., Boschini, F., Traina, K., Bontempi, S., Remy, J. C., Cloots, R., & Vandewalle, N. (2012). Measuring the flowing properties of powders and grains. *Powder Technology*, 224, 19–27. https://doi.org/10.1016/j.powtec.2012.02.015
- Magasiner, N., Van Alphen, C., Inkson, M. B., & Misplon, B. J. (2002). Characterising fuels for biomass - Coal-fired cogeneration. *International Sugar Journal*, 104(1242), 251–267.
- Mendonça, F. G. de, Cunha, I. T. da, Soares, R. R., Tristão, J. C., & Lago, R. M. (2017). Tuning the surface properties of biochar by thermal treatment. *Bioresource Technology*, 246(May), 28–33. https://doi.org/10.1016/j.biortech.2017.07.099
- Mousa, E. A., Babich, A., Senk, D., Metallurgy, F., & Aachen, R. (2015).
 Iron Ore Sintering Process with Biomass Utilization E A Mousa,
 A Babich, D Senk, Institute of Ferrous Metallurgy Iron Ore
 Sintering Process with Biomass Utilization. METEC and 2nd

- ESTAD, Düsseldorf, 15 19 June 2015, 1–13.
- Mu, L., Wang, R., Xie, P., Li, Y., Huang, X., Yin, H., & Dong, M. (2023). Comparative investigation on the pyrolysis of crop, woody, and herbaceous biomass: Pyrolytic products, structural characteristics, and CO 2 gasification. *Fuel*, 335(November 2022), 126940. https://doi.org/10.1016/j.fuel.2022.126940
- Mudryk, K., Jewiarz, M., Wr, M., Niemiec, M., & Dyjakon, A. (2021).
 Evaluation of Urban Tree Leaf Biomass-Potential, Physico-Mechanical and Chemical Parameters of Raw Material and Solid Biofuel.
 Energies, 14(818), 1–14.
 https://doi.org/10.3390/en14040818
- Nugraha, S. S., Sartohadi, J., & Nurudin, M. (2022). Field-Based Biochar, Pumice, and Mycorrhizae Application on Dryland Agriculture in Reducing Soil Erosion. Applied and Environmental Soil Science, 2022. https://doi.org/10.1155/2022/1775330
- Oginni, O., & Singh, K. (2019). Pyrolysis characteristics of Arundo donax harvested from a reclaimed mine land. *Industrial Crops and Products*, 133(March), 44–53. https://doi.org/10.1016/j.indcrop.2019.03.014
- Omoniyi, P., Ibitoye, S., Popoola, O., Ikubanni, P., Adeleke, A., Mahamood, M., Jen, T. C., & Akinlabi, E. (2023). Recycling Plastic Waste as Composite Reinforcement. *E3S Web of Conferences*, 430, 8–12. https://doi.org/10.1051/e3sconf/202343001298
- Ong C.K., Ghazali N.F., Hasbullah H., Ismail A.F., Rahman S.A., Kusworo T.D., Lee C.T. (2024). Biomass-Based Biochar as Adsorbent: a Mini Review of Production Methods, Characterization, and Sustainable Applications. *Chemical Engineering Transactions*, 113, pp. 493 498. https://doi.org/10.3303/CET24113083
- Osman, A. I., Fawzy, S., Farghali, M., El-Azazy, M., Elgarahy, A. M., Fahim, R. A., Maksoud, M. I. A. A., Ajlan, A. A., Yousry, M., Saleem, Y., & Rooney, D. W. (2022). Biochar for agronomy, animal farming, anaerobic digestion, composting, water treatment, soil remediation, construction, energy storage, and carbon sequestration: a review. *Environmental Chemistry Letters*, 20(4), 2385–2485. https://doi.org/10.1007/s10311-022-01424-x
- Oyebamiji, O. O., Olaleru, A. S., Oyeleke, R. B., & Ofodile, L. N. (2025). Evaluation and characterization of biochar and briquettes from agricultural wastes for sustainable energy production. *Waste Management Bulletin*, *3*(3), 100198. https://doi.org/10.1016/j.wmb.2025.100198
- Parikh, J., Channiwala, S. A., & Ghosal, G. K. (2007). A correlation for calculating elemental composition from proximate analysis of biomass materials. *Fuel*, 86(12–13), 1710–1719. https://doi.org/10.1016/j.fuel.2006.12.029
- Pariyar, P., Kumari, K., Jain, M. K., & Jadhao, P. S. (2020). Evaluation of change in biochar properties derived from different feedstock and pyrolysis temperature for environmental and agricultural application. *Science of the Total Environment*, 713, 136433. https://doi.org/10.1016/j.scitotenv.2019.136433
- Patil, Y., Ku, X., & Vasudev, V. (2023). Pyrolysis Characteristics and Determination of Kinetic and Thermodynamic Parameters of Raw and Torrefied Chinese Fir. ACS Omega, 8(38), 34938–34947. https://doi.org/10.1021/acsomega.3c04328
- Pattanayak, S., & Loha, C. (2023). Investigation of kinetic triplets and thermodynamic parameters of different species of bamboobiomass from North-East India. *International Journal of Chemical Kinetics*, March, 335–349. https://doi.org/10.1002/kin.21639
- Pattanayak, S., Loha, C., Kumar Singh, R., & Saha, D. (2023). Experimental investigation of thermal performance, kinetic triplets, and synergistic effect for bamboo-waste plastic (PP & PE) blends using thermogravimetric analyser in N2 atmosphere. Sustainable Energy Technologies and Assessments, 57(May), 103266. https://doi.org/10.1016/j.seta.2023.103266
- Pohlmann, J. G., Borrego, A. G., Osório, E., Diez, M. A., & Vilela, A. C. F. (2016). Combustion of eucalyptus charcoals and coals of similar volatile yields aiming at blast furnace injection in a CO2 mitigation environment. *Journal of Cleaner Production*, *129*, 1–11. https://doi.org/10.1016/j.jclepro.2016.04.138
- Putri, U. M., Sarifuddin, & Bintang. (2023). Characteristic of Mahogany leaves as biochar and its effect with Urea fertilization on nitrogen status and growth of corn in Ultisol. *IOP Conference Series: Earth and Environmental Science*, 1241(1). https://doi.org/10.1088/1755-1315/1241/1/012025

- Qiu, L., Li, C., Zhang, S., Wang, S., Li, B., Cui, Z., Tang, Y., & Hu, X. (2023). Distinct property of biochar from pyrolysis of poplar wood, bark, and leaves of the same origin. *Industrial Crops and Products*, 202(June), 117001. https://doi.org/10.1016/j.indcrop.2023.117001
- Rajendra, I. M., Winaya, I. N. S., Ghurri, A., & Wirawan, I. K. G. (2019). Pyrolysis study of coconut leaf's biomass using thermogravimetric analysis Pyrolysis study of coconut leaf's biomass using thermogravimetric analysis. *IOP Conf. Series: Materials Science and Engineering*, 539, 012017. https://doi.org/10.1088/1757-899X/539/1/012017
- Safarian, S. (2023). To what extent could biochar replace coal and coke in steel industries? *Fuel*, *339*(December 2022), 127401. https://doi.org/10.1016/j.fuel.2023.127401
- Satomi, I. M., Mustafa, B. G., Mohammed, H. D., Abdulaziz, L., & Silas, K. (2025). Biochar Production from Leave Biomass for Environmental Sustainability and Applications. *Chem. Res. Tech.* 2, 12–18. https://www.chemrestech.com/article_213888_2fee631450cfb 6787c8477223d026819.pdf
- Selvarajoo, A., & Oochit, D. (2020). Effect of pyrolysis temperature on product yields of palm fibre and its biochar characteristics. *Materials Science for Energy Technologies*, 3, 575–583. https://doi.org/10.1016/j.mset.2020.06.003
- Singh, K. R., Sarkar, A., & Chakraborty, P. J. (2019). Effect of torrefaction on the physicochemical properties of pigeon pea stalk (Cajanus cajan) and estimation of kinetic parameters. *Renewable Energy*, 138, 805–819. https://doi.org/10.1016/j.renene.2019.02.022
- Singh, S., Chakraborty, J. P., & Mondal, M. K. (2020). Torrefaction of woody biomass (Acacia nilotica): Investigation of fuel and flow properties to study its suitability as a good quality solid fuel. Renewable Energy, 153, 711–724. https://doi.org/10.1016/j.renene.2020.02.037
- Spokas, K. A. (2010). Review of the stability of biochar in soils: Predictability of O:C molar ratios. *Carbon Management*, 1(2), 289–303. https://doi.org/10.4155/cmt.10.32
- Stylianou, M., Christou, A., Dalias, P., Polycarpou, P., Michael, C., Agapiou, A., Papanastasiou, P., & Fatta-Kassinos, D. (2020). Physicochemical and structural characterization of biochar derived from the pyrolysis of biosolids, cattle manure and spent coffee grounds. *Journal of the Energy Institute*, 93(5), 2063–2073. https://doi.org/10.1016/j.joei.2020.05.002
- Szalay, A., Kelemen, A., & Pintye-Hódi, K. (2015). The influence of the cohesion coefficient (C) on the flowability of different sorbitol types. *Chemical Engineering Research and Design*, 93(May), 349– 354. https://doi.org/10.1016/j.cherd.2014.05.008
- Tan, M. (2023). Conversion of agricultural biomass into valuable biochar and their competence on soil fertility enrichment. *Environmental Research*, 234(June), 116596. https://doi.org/10.1016/j.envres.2023.116596
- Tannous, K., Lam, P. S., Sokhansanj, S., & Grace, J. R. (2013). Physical properties for flow characterization of ground biomass from douglas fir wood. *Particulate Science and Technology*, 31(3), 291– 300. https://doi.org/10.1080/02726351.2012.732676
- Trif-Tordai, G., & Ionel, I. (2011). Waste Biomass as Alternative Bio-Fuel
 Co-Firing versus Direct Combustion. In M. Manzanera (Ed.),
 Alternative Fuel (pp. 285–306). Intechopen.
 https://doi.org/10.5772/25030
- UN. (2024). Take Action for the Sustainable Development Goals. UN Sustainable Development Goals. https://www.un.org/sustainabledevelopment/sustainabledevelopment-goals/
- Wojtacha-Rychter, K., & Smoliński, A. (2019). A study of dynamic adsorption of propylene and ethylene emitted from the process of coal self-heating. *Scientific Reports*, 9(1), 1–15. https://doi.org/10.1038/s41598-019-54831-6
- Wu, X. F., Li, S. X., & Li, M. F. (2019). Effect of temperature on the properties of charcoal prepared from carbonization of biorefinery lignin. *BioResources*, 13(3), 6736–6745. https://doi.org/10.15376/biores.13.3.6736-6745
- Yang, H., Yan, R., Chen, H., Lee, D. H., & Zheng, C. (2007). Characteristics of hemicellulose, cellulose and lignin pyrolysis. Fuel, 86(12–13), 1781–1788. https://doi.org/10.1016/j.fuel.2006.12.013
- Yiga, V. A., Lubwama, M., & Olupot, P. W. (2023). Pyrolysis, kinetics

and thermodynamic analyses of rice husks/clay fiber-reinforced polylactic acid composites using thermogravimetric analysis. *Journal of Thermal Analysis and Calorimetry*, *148*(9), 3457–3477. https://doi.org/10.1007/s10973-022-11927-y

Zhang, A., Liu, Y., Pan, G., Hussain, Q., Li, L., Zheng, J., & Zhang, X. (2012). Effect of biochar amendment on maize yield and greenhouse gas emissions from a soil organic carbon poor

calcareous loamy soil from Central China Plain. *Plant and Soil*, 351(1–2), 263–275. https://doi.org/10.1007/s11104-011-0957-x Zhao, S. X., Ta, N., & Wang, X. D. (2017). Effect of temperature on the structural and physicochemical properties of biochar with apple tree branches as feedstock material. *Energies*, 10(9). https://doi.org/10.3390/en10091293



© 2025. The Author(s). This article is an open access article distributed under the terms and conditions of the Creative Commons Attribution-ShareAlike 4.0 (CC BY-SA) International License (http://creativecommons.org/licenses/by-sa/4.0/)